Proc. Natl. Acad. Sci. USA
Vol. 90, pp. 10489–10493, November 1993
Biochemistry

Topography of the histone octamer surface: Repeating structural motifs utilized in the docking of nucleosomal DNA

(histone fold/helix–strand–helix motif/parallel β bridge/binary DNA binding sites/nucleosome)

GINA ARENTS* AND EVANGELOS N. MOUDRIANAKIS*†

*Department of Biology, The Johns Hopkins University, Baltimore, MD 21218; and †Department of Biology, University of Athens, Athens, Greece

Communicated by Christian B. Anfinsen, August 5, 1993

ABSTRACT **The histone octamer core of the nucleosome is a protein superhelix of four spirally arrayed histone dimers. The cylindrical face of this superhelix is marked by intradimer and interdimer pseudodyad axes, which derive from the nature of the histone fold. The histone fold appears as the result of a tandem, parallel duplication of the "helix–strand–helix" motif. This motif, by its occurrence in the four dimers, gives rise to repetitive structural elements—i.e., the "parallel β bridges" and the "paired ends of helix I" motifs. A preponderance of positive charges on the surface of the octamer appears as a left-handed spiral situated at the expected path of the DNA. We have matched a subset of DNA pseudodyads with the octamer pseudodyads and thus have built a model of the nucleosome. In it, the two DNA strands coincide with the path of the histone-positive charges, and the central 12 turns of the double helix contact the surface of the octamer at the repetitive structural motifs. The properties of these complementary contacts appear to explain the preference of histones for double-helical DNA and to suggest a possible basis for allosteric regulation of nucleosome function.**

The genetic material of eukaryotic cells is compacted initially ≈6-fold by its association with the four core histones H2A, H2B, H3, and H4 and the linker histone H1 to form the 100-Å-diameter fiber of chromatin. This fiber enters into several cascaded levels of compaction that culminate in the microscopically visible chromosome, with overall DNA compaction $\approx 10^4$-fold. The 100-Å chromatin fiber comprises a string of repeating units (1) called nucleosomes (2), in which a stretch of DNA is wound around one core histone octamer $(H2A,H2B,H3,H4)_2$. Recently, we have solved the structure of the octamer by single crystal x-ray crystallography at 3.1-Å resolution (3) and found it to be tripartite—i.e., a centrally located $(H3\text{-}H4)_2$ tetramer is flanked by two H2A-H2B dimers. The three subunits are assembled in the form of a left-handed protein superhelix with an apparent pitch of 28 Å and form a solid object with a small central cavity. This object is bounded by two apposing, nonparallel faces that rest on the rims of a rather smooth cylindrical surface—i.e., the histone octamer resembles a cylindrical wedge.

Here we present the results of our analysis of the surface topography of the histone octamer. This analysis allowed us to identify fundamental components of the histone fold, which through various symmetry operations yield repeating structural elements on the cylindrical face of the octamer that match certain symmetries of the DNA double helix. Next, we used these findings to dock double-stranded DNA on the cylindrical face of the octamer and generated a model for the nucleosome. Finally, we present newly identified DNA–protein binding motifs and non-sequence-specific patterns of interactions. The model offers strong predictive criteria for structural and genetic biology.

METHODS

The determination of the structure of the histone octamer at 3.1 Å has been described (3). The overall shape and volume of this tripartite structure is in agreement with the results of three independent studies based on differing methodologies—i.e., x-ray diffraction, neutron diffraction, and electron microscopic image reconstruction (4–6). Furthermore, the identification of the histone fold, a tertiary structure motif of ≈65 residues found in all four core histones, is additional evidence of the correctness of the structure. We have extended the model for H2A from its previously reported end at residue 109 to include residues 110–115.

By close inspection of the model and by use of internal true symmetries and local pseudosymmetries, we have identified a number of structural landmarks on the cylindrical face of the octamer. They appear with regularity, and their spacing on that surface is reminiscent of the periodicities of DNA–protein contacts in the nucleosome. Furthermore, in modeling the nucleosome we have used the following constraints. The DNA is wrapped on the outside of the histone core (7). Since the double helix is 20 Å wide and the protein superhelical path is narrow, particularly at the apex of the wedge (10 Å), there is not much space for lateral displacement of the double helix before it loses its contacts with the protein. In addition, the results of the nuclease digestion (8) and hydroxyl radical footprinting studies (9) help to position the DNA relative to the histone masses in the octamer and to fix its variations in twist within narrow limits. Finally, the minor groove has been shown to face directly outward at the protein twofold axis (4). These constraints define a DNA path rather precisely, permitting only small-scale adjustments of local deformations of the double helix—e.g., kinks, etc. To this end, a uniformly bent 146-bp DNA was generated by using DNABEND (10). The central 30 bp were constrained to a twist of 10.7 bp per turn, the outer 116 bp were constructed with 10.0 bp per turn (9), and all were set to a supercoil of 28-Å pitch and 105-Å average outer diameter. This initial model was fitted to the protein backbone of the histone octamer surface by using FRODO (11) as implemented on a MicroVAX II and Evans and Sutherland PS390, following the constraints outlined above. Kinks were formed at the locations of approximately ±1 and ±4 helical turns (4), and additional small bends were added to improve the fit of the DNA to the protein. Since only C^α coordinates were used, energy minimization operations have been postponed until after the octamer structure is refined. Illustrations of the model were made with the programs FRODO and MIDAS (12) on a Silicon Graphics (Mountain View, CA) Personal Iris.

The publication costs of this article were defrayed in part by page charge payment. This article must therefore be hereby marked "*advertisement*" in accordance with 18 U.S.C. §1734 solely to indicate this fact.

Abbreviations: PEM, paired-element motif; PEH, paired ends of helices.

[Note that we frequently refer to termini of the histones and to ends of α-helices. "Terminus(ni)" refers to the natural N- or C-terminal section of the entire chain, while "amino end" and "carboxyl end" are used to describe local directions of a defined segment of a helix.]

RESULTS

Footprints of the Histones on the Octamer Surface. We showed earlier that the histone octamer is a cylindrical wedge that is derived from the spiral assembly of the four histone dimers into a left-handed protein supercoil. Within this supercoil, each dimer subtends an arc of 140° on the cylindrical face of the octamer. Within each dimer the histone chains are not folded as individual globular entities, as previously assumed, but have an extended conformation; each folded chain clasps its partner in a characteristic handshake motif (3). Consequently, the resulting superhelical surface has a complex topography to which each histone chain contributes a minimum of two distinct, separate domains (Fig. 1). Starting at the outermost point along the histone cylinder and traveling in a spiral path of 28-Å pitch toward the twofold axis at the "front" of the tetramer, the structured portions of the histones emerge on the surface in the following order: first $H2A^1$; then $H3^2$, $H2A^1$, $H2B^1$, $H2A^1$, $H2B^1$, $H4^1$, $H3^1$, $H4^1$, and finally $H3^1$-$H3^2$ overlapping at the zero position. As discussed later, due to the distance between the two phosphodiester backbones across the DNA helix, the order in which the histone domains appear on the octamer surface is not necessarily the order in which they are contacted by an individual strand of the double helix.

Closer examination of the cylindrical face of the wedge reveals a number of repeating motifs of quaternary organization of the histone chains, a direct consequence of the histone fold and its head-to-tail packaging within the histone dimers (3). The histone fold, the common feature of the four core histones, consists of a short α-helix (I; ≈10 residues) followed by a loop and β-strand segment (strand A), a long helix (II; ≈27 residues), another short loop and β-strand segment (strand B), and a final short helix (III; ≈10 residues). Thus, the histone fold appears as a tandem, parallel duplication of a fundamental element, the helix–strand–helix motif, with the junction point near the middle of the long helix II. It should be noted that three of the four histones have extra fold helical sections located on the amino or the carboxyl side of the fold and we refer to them, respectively, as N helix or C helix.

Paired-Element Motifs (PEMs). The helix–strand–helix motif occurs 2 times in each chain and 16 times in the entire octamer. In the head-to-tail association of the histones within each dimer, strand A from one chain runs parallel to strand B from the other chain to form a parallel β bridge (Fig. 2*A*), two per dimer. All eight of these parallel β bridges are located on the cylindrical face of the octamer.

A different type of repeating quaternary structure element is formed at the cylindrical face of the octamer by the local juxtaposition of the amino ends of helix I from each of the histone dimer partners. This, which we call the "paired ends of helices" (PEH) motif, occurs at the midpoint of the surface that each dimer exposes on the octamer superhelical face.

Comparison of Octamer and DNA Symmetries. The cylindrical face of the histone octamer is pierced by pseudotwofold axes that can be matched with a select subset of the pseudodyads of the DNA double helix. The first set derives from the head-to-tail packaging of two histone folds within each dimer. Each histone dimer has a pseudodyad exactly halfway along its footprint on the superhelical surface—i.e., in the middle of the PEH motif. The second set of pseudodyads relates one whole dimer to the next—i.e., they bisect the interfaces between dimers. These result in a total of seven symmetry axes on the cylindrical surface of the octamer. The structure of DNA allows the placement of pseudodyads exactly in the middle of either the major or the minor groove, either in the plane of a base pair or halfway between adjacent base pairs. If the protein superhelix is unrolled and placed parallel to a DNA double helix, the protein pseudodyads can be aligned to coincide with a select subset of DNA pseudodyads emanating from the minor groove. As a result, a very simple and strongly suggestive image emerges (Fig. 2*B*) in which the minor groove of the DNA helix makes a finite number of periodic contacts with the surface of the protein superhelix. Guided by this striking complementarity between the protein and DNA pseudosymmetries, we model-built the nucleosomal DNA phosphodiester backbone in a manner that

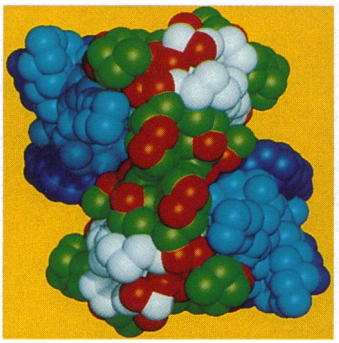

FIG. 1. Footprints of histones on octamer surface. Each chain contributes to at least two well-separated areas of the octamer surface. The C^α positions of arginine and lysine residues of the tetramer are highlighted red. View is down the molecular twofold axis. Surfaces were calculated from C^α positions at twice the van der Waals radii; H3 is green, H4 is white, H2A is light blue, and H2B is dark blue.

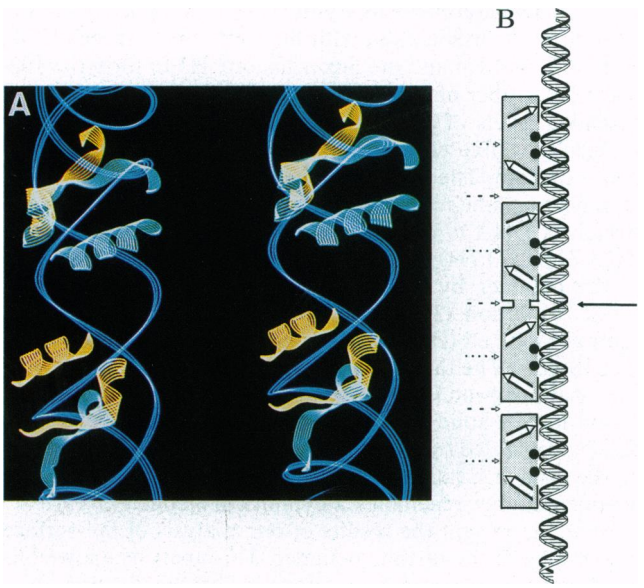

FIG. 2. PEMs. (*A*) Stereoview of a ribbon representation of the PEMs in one H3-H4 dimer relative to the DNA. Three PEMs are seen; the central two helices constitute the single PEH motif while the two pairs of β strands are the two parallel β bridges. This pattern repeats in each of the four histone dimers. H3 is yellow, H4 is light blue, and the DNA path is dark blue. (*B*) Linearized view of the histone–DNA interface, showing the superposition of their symmetries. Each shaded box represents a histone dimer. In it, two parallel lines represent a parallel β bridge, with the arrowhead pointing in the N to C direction. Pair of black circles indicates position of the PEH motif. Dotted and dashed lines represent intradimer and interdimer pseudodyads, respectively.

would also incorporate relevant information on histone–DNA contacts derived from earlier studies. The resulting model has aided us in identifying histone–DNA binding motifs and the possible role of the unstructured, highly charged histone termini in nucleosome assembly and regulation.

Octamer Surface Elements Involved in DNA Docking. The model of the nucleosome shown in Fig. 3 has the overall shape of a short cylinder 105 Å in diameter and 65 Å long. In accordance with earlier nomenclature (6, 13), the contact between DNA and the surface of the octamer at the point where the two molecules of H3 meet at the molecular twofold axis is referred to as zero. The turns of the advancing DNA double helix are numbered from −7 to +7, before and after the zero point, respectively. In our model, the 14-turn DNA helix makes contact with 14 patches of the octamer surface. For the central 12 patches (from −5.5 to +5.5) the contact surface is rather large, while for the outer 2 patches (at ±6.5) the contact area is significantly smaller.

If a single strand of the modeled DNA is followed from the 5′ to the 3′ end, the backbone makes the following *primary* contacts with the octamer surface: $H3^2$, $H2B^1$, $H2A^1$, $H2B^1$, $H3^1$, $H4^1$, $H3^1$, $H4^2$, $H3^2$, $H4^2$, $H2A^2$, $H2B^2$, $H2A^2$, and $H3^1$. This order is in good agreement with the findings of Bavykin *et al.* (14). It should be compared to the order in which the structured portions of the histones emerge along the same spiral path (see *Footprints of the Histones on the Octamer Surface*).

Repeating DNA Binding Motifs. There are two levels of repeating protein–DNA interactions in our model: (*i*) those arising from repeating elements of the three-dimensional structure within each histone dimer, and (*ii*) those due to patterns of certain types of side chains on the cylindrical face of the octamer.

Repeating structural motifs. The parallel β bridges are three-dimensional landmarks of each histone dimer surface. Eight of the 12 protein patches where the DNA backbone touches the cylindrical surface of the octamer (Fig. 3*B*) contain the parallel β bridge elements, and the remaining four contacts are formed with the PEH motifs. Each histone dimer contains three DNA binding sites, two β bridge motifs, and a single PEH element bisecting the arc between the bridges.

In each histone, the loop immediately preceding strand B of the β bridge has two invariantly positively charged residues, usually Lys-Arg (but Lys-Lys in H2A). Although the chemical nature of the side chains on the β bridges varies from histone to histone and from strand A to strand B, the beginning of the β bridge binding site is always marked by the two invariant positive charges.

The amino ends of α-helices have positive dipole moments associated with them (15). In the histone octamer, there are 32 α-helices, and 28 of these have their amino ends pointing toward the superhelical surface. In addition to the amino ends of helices I (see above), the amino ends of helices II and III, found at the carboxyl end of the β bridges, also point directly toward the nearby DNA backbones. Finally, the amino ends of the N helices of H2A and H3 also lie close to the phosphodiester backbones (Fig. 4). The pattern of these positive dipole ends aligned on the octamer surface suggests that they could contribute to "steering" and docking the DNA.

Repeating chemical motifs. Three types of amino acids are found at the DNA binding sites. First, as expected, there are many positively charged residues along the entire DNA binding surface. As the phosphodiester backbones writhe periodically over the protein surface, three phosphate groups per strand per turn come within interaction distance with the protein. Lysines and arginines are generally found at the edges of these sites, where, due to their side-chain length, they can make contacts with the first or last of the three phosphate groups (Fig. 4). The second type of amino acid, the hydroxyl-containing residues, are generally well positioned to make contact with the most central of the three close-approach phosphates. Usually, these residues are serines or threonines and are located near the center of the β bridge; less frequently they are found at the amino end of helix I. The third, less common, type of residues found in DNA binding locations are the hydrophobic residues: Ile-79 (H2A); Ile-39, Tyr-40, and -42 (H2B); Leu-65 and Met-120 (H3); and possibly Leu-49 (H4). Electron densities for the side chains of these residues extend from the histone superhelical surface and appear to lie slightly inside both grooves of the double helix. The tyrosines of H2B appear to have the potential for a dual role; their aromatic rings protrude slightly into the DNA grooves, suggesting possible hydrophobic interactions, and their hydroxyl groups are well positioned to form hydrogen bonds with phosphate oxygens.

Nonrepeating DNA binding sites. All four core histones have residues both before and after the common fold. The

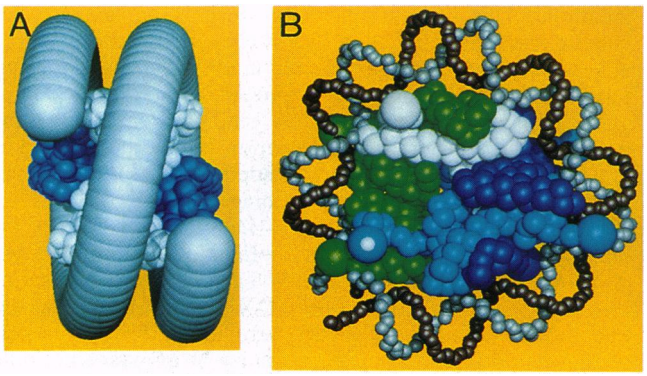

FIG. 3. Nucleosome model. (*A*) View is down the molecular twofold axis; DNA is represented by a 20-Å tube that almost completely occludes the protein. (*B*) View is down the superhelical axis; only the backbone atoms of the DNA double helix are shown. The order in which the histones contribute to this side of the octamer surface can be followed (compare to Figs. 1 and 5; same color codes) as well as the order in which the histones are encountered by an individual strand of DNA.

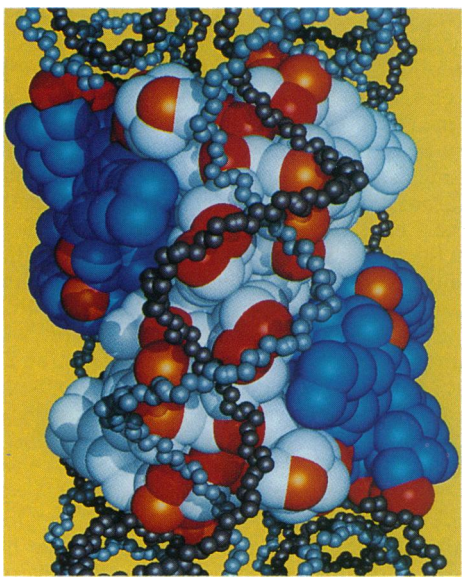

FIG. 4. Coincidence of positive charges and DNA track. The H3-H4 tetramer is white, the H2A-H2B dimers are blue. The C^{α} atoms of lysines and arginines on the cylindrical surface are red, and atoms indicating the positions of the positive dipole ends of helices are orange. Atoms of the DNA backbone are undersized to allow visualization of the protein surface. View is as in Fig. 3*A*.

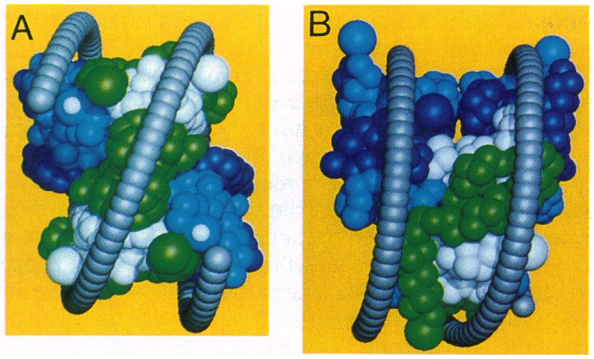

FIG. 5. Origins of flexible histone termini. The histone octamer wrapped by a thin (10 Å) tube that represents the projection of the DNA helix axis onto the cylindrical face of the octamer, while allowing visualization of the protein features. Locations of the proximal ends of the labile termini in the model are marked by 7-Å-radius spheres placed next to the last well-ordered residue of each chain. Color code is that of Fig. 1; the carboxylmost residue of H2A is marked by a blue-with-white dot indicator. (*A*) View is down the molecular twofold axis. (*B*) The plane of the paper contains both the molecular twofold and the superhelical axes. See Fig. 3*B* for a view down the superhelical axis.

extrafold N helices of H3 and H2A and the C helix of H2B appear to make significant contributions to DNA binding. The N helix of H2A and the carboxyl end of the C helix of H2B partially protrude past the gyres of the DNA supercoil (Fig. 5) and set an outside limit to the path of the supercoil on the H2A-H2B dimers. The first six imaged residues of H2A (residues 15–20) and the last seven residues of H2B (residues 119–125) contain exclusively positively charged or hydroxyl-containing amino acids; thus, they are highly likely to be important in DNA binding. In our model, residues on the N helix of H3 (Arg-49, -52, and -53; Lys-55) make the final contacts with the entering and exiting nucleosomal DNA in the region of the twofold axis (Fig. 5), in agreement with earlier findings (14). The C terminus of H2A (residues 107–115) also runs along the flat side of the tetramer toward the zero position but is shielded by H3 from contact with the nucleosomal core DNA; therefore, the contacts found earlier (14) between H2A and the entering and exiting DNA are probably due to the final (unimaged) 13 residues.

Alternating structural motifs. In general, the origins of the flexible ends of the histone chains are found on alternating sides of the DNA path (see Fig. 5). Specifically, starting from the entry point of the DNA on the nucleosome model, and progressing in a left-handed spiral, the DNA encounters first $H2A^1$ (carboxyl-most end) on the outside of the path, then the amino-most ends of $H3^2$ on the inside, $H2B^1$ on the inside, $H2A^1$ on the outside, $H2B^2$ on the inside, $H4^1$ on the outside, and, finally, nearest the zero position, $H3^1$ on the inside. This sequence is inverted for the other half of the path. Since the termini are not represented in our structure, we have no information on which (or how many) DNA strand(s) a given terminus contacts, but the locations of the ends that we see present a balanced, alternating pattern of histone chain end contacts with the double helix.

DISCUSSION

The analysis of the surface architecture of the histone octamer core of the nucleosome has revealed several hitherto unknown structural motifs and organizational patterns that advance our understanding of gene structure and regulation. A possible role of pseudosymmetries in nucleosome organization has been suggested earlier (16), but the specifics of that insightful proposal differ from the current experimental observations. The analysis we present here was based almost exclusively on information derived from the C^{α} backbone of our 3.1-Å octamer structure. The most notable feature of this object is the organization of its cylindrical face which, at ≈5-Å detail, is impressively smooth and continuous but not featureless. It is not marked by any sharp protrusions reminiscent of the elbows, fingers, or kinks of other (sequence recognizing) DNA binding proteins (17). However, it is marked 12 times, over 560°, by the repeated and symmetrical presence of two types of PEMs—i.e., the parallel β bridges and the PEHs extending to this surface. These elements derive from the two tandemly repeated helix–strand–helix motifs of the histone fold. Its repetitive occurrence in all four core histone chains leads us to propose that this motif may be the common precursor to all core histones. If so, the histone fold can be considered the result of a tandem, parallel duplication of a single archetypal gene specifying a DNA binding protoprotein and selected for its dimerization potential.

The footprint of each dimer on the superhelical surface is exactly long enough to interact with three full turns of the DNA double helix. The primary interactions appear to involve mainly the ribosyl phosphate backbone, since the histone chains clearly do not form 2° and 3° elements that extend beyond the average surface of the octamer. The spiral arrangement of the four dimers within the octamer yields a periodic appearance of the 12 PEMs on the cylindrical face of the octamer. This periodicity coincides with the known periodic contacts of the DNA supercoil with the histone octamer surface (4, 9, 14)—i.e., contacts are made every full turn of the DNA double helix.

The primary histone–DNA contacts in our model are balanced on the two sides of the double helix. Each histone chain in a dimer contributes to all three of the DNA binding sites within that dimer, and thus both dimer partners make analogous contributions to the binding of each DNA strand. An individual strand of DNA will interact primarily with one of the histones in two places and with the other histone only once. This pattern inverts at the symmetry-related dimer. For example, if one strand of DNA as it encounters the $H3^1$-$H4^1$ dimer first interacts with $H3^1$, at the next turn of the double helix this strand will touch $H4^1$, and at the third turn of the helix, it will again interact with $H3^1$. The inverse pattern is seen on the symmetry-related $H3^2$-$H4^2$ dimer, where the same strand contacts $H4_2$, then $H3_2$, and finally $H4_2$ again. The other strand of DNA establishes the same alternating pattern but in the reverse order. H2A and H2B make similar, alternating contacts, at opposite ends of the octamer. This pattern suggests that modifications in a single histone might generate changes in the nucleosome at several widely spaced locations. This suggestion evokes serious implications for genetic regulation and allows for the prediction of a position effect for certain posttranslational modifications and/or mutations in a select subset of histone sites.

The existence of paired DNA binding elements on the octamer offers a possible explanation for the preference of the core histones for double-stranded DNA. First, the elements of the primary DNA binding sites of the octamer (PEMs) have a binary character—i.e., they are formed by pairing of analogous structural motifs. In addition, the two units in each pair are separated by a distance appropriate for the simultaneous binding of both DNA strands at that locus. Second, these PEMs are spirally arrayed on the convex side of the cylindrical face of the octamer in an exact periodic pattern. The apposing, concave side of the nucleosomal DNA spiral presents to the protein a pattern of binary and periodically spaced potential docking sites (the turns of the double helix); their periodicity is complementary to that of the protein. As the macromolecules search for docking, the degree of complementation between these two groups of multisite binary patterns will set the criteria for the fidelity of, and the energetic advantage for the selection among, poten-

tial docking partners. Both of these parameters become optimized by the association of the octamer with double- rather than single-stranded DNA or RNA. Thus, the avidity of histone octamers for DNA is the result of docking optimization of two complementary stereochemical arrays, and its strength derives from the additive contributions of repetitive favorable interactions. This arrangement provides a sequence-independent yet region-specific and exact coupling of the two complementary polymeric surfaces.

The symmetry of repeating DNA binding elements on the surface of the octamer strongly suggests that the number of base pairs between one DNA binding site and the next should be an integer—i.e., very close to 10.0 or 11.0. For the protein and DNA pseudodyads to coincide, the phosphates must be presented to similar sites of the protein surface in approximately the same orientation. Therefore, in building the nucleosome model, we easily fitted DNA with a twist of 11 bp per turn across the protein surface from position -0.5 to $+0.5$. In the two adjacent turns of the double helix (± 0.5 to ± 1.5), the change in the angle at which the double helix approached the protein surface caused the most "inaccessible" base in the DNA at ± 1.5 to be 10 bases away on one strand and 11 bases away on the other, for a total 2-bp change in the apparent twist over the central three turns. For the rest of the DNA model, a twist of 10 bp per turn was consistent with optimum DNA proximity to the paired element motifs.

In a histone dimer, the last ordered residues proximal to the labile N termini are contacting opposite sides of the DNA double helix. Dimensional constraints of the model prevent the threading of the histone terminal residue sections between the protein and DNA faces (Fig. 3*B*). Our model does not provide clues as to which (or how many) of the nearby gyres of DNA each terminus might bind. However, even if both of the highly positively charged termini from one dimer interact with the same gyre of DNA, they must do so from opposite sides of the double helix. This requires that at least one terminus, and probably both termini, of a dimer must be freed from the nucleosomal DNA whenever the transcription or replication assemblies are processing the DNA, and this invokes a regulatory role for the termini.

CONCLUSION

From an architectural standpoint, the octamer is a quaternary assembly of four modules—i.e., the histone dimers (3). We have presented here clear evidence for the existence of intradimer and interdimer symmetries that emanate from the properties of the histone fold. Related to these symmetries are 12 PEMs, which together with the two ends of the entire protein superhelix yield 14 structural landmarks regularly spaced around the octamer. They constitute the protein docking pads for each of the consecutive 14 contacts the double helix makes in our nucleosome model.

From a thermodynamic standpoint, the octamer is a tripartite, dynamic protein assembly governed by positive cooperativity and reversibility (3, 18). However, when the octamer is functioning in an array of nucleosomes, the dynamics of the system must be seriously altered. Steric and topological constraints imposed by the wrapping of the double helix around the octamer (Fig. 3*A*) are expected to modulate both the energetics and the kinetics of its assembly. It is clear that, in the process of nucleosome disassembly, the octamer cannot escape from the DNA supercoil as a single unit; it must first "untwist" along the dimer–tetramer interface in a concerted fashion with the opening of the DNA supercoil. Subsequently, if the proteins are to leave the DNA, the dimers will be the first subunits to separate and dissociate before the tetramer can leave the DNA of an unfolded nucleosome. What still remains unclear is the time resolution of the anticipated steps.

From an evolutionary viewpoint, it appears that the problem of DNA–histone interactions was solved once at the level of the histone dimer by the advent of the histone fold. The most advanced expression of this solution is found in the eukaryotic histone octamer, but simpler protein assemblies with analogous DNA-folding properties have been reported—i.e., of the HU type (ref. 13, pp. 168–172) and HMf (19). It will be interesting to know whether such proteins also contain the histone fold.

The unique character of the histone octamer as a DNA compacting spool stems from its organization into three thermodynamic modules, which, through independent chemical modifications, and by virtue of their relative ease of reversible assembly, offer to the system great flexibility for regulation. In contrast, while a monolithic protein spool can be envisioned with the same overall DNA binding properties, such a "plinth" would have been subjected to negative selective pressures due to serious limitations (steric and energetic) of its regulation potential. So, although the histone octamer is indeed a spool of DNA compaction, it appears that the intricacies of its structure have been so selected as to make it a modular, dynamically balanced scaffold that can function as a "gene endoskeleton." When it is the target of various chemical and structural alterations, this articulated spool, by evoking coupled allotopic (from Greek: allos, different; topos, place) conformational transitions, becomes an allosteric effector. As such, it can function simultaneously as substrate and mediator of genetic regulation.

We are grateful to Drs. Mario Amzel and George Scangos for their critical reading of the manuscript. This work was supported in part by the Biology Department of The Johns Hopkins University and by the kind donations of several friends, especially Drs. George and Leslie Scangos of Miles Pharmaceuticals.

1. Kornberg, R. D. (1974) *Science* **184**, 868–871.
2. Oudet, P., Gross-Bellard, M. & Chambon, P. (1975) *Cell* **4**, 281–300.
3. Arents, G., Burlingame, R. W., Wang, B.-C., Love, W. E. & Moudrianakis, E. N. (1991) *Proc. Natl. Acad. Sci. USA* **88**, 10148–10152.
4. Richmond, T. J., Finch, J. T., Rushton, B., Rhodes, D. & Klug, A. (1984) *Nature (London)* **311**, 532–537.
5. Bentley, G. A., Lewit-Bentley, A., Finch, J. T., Podjarny, A. D. & Roth, M. (1984) *J. Mol. Biol.* **176**, 55–75.
6. Klug, A., Rhodes, D., Smith, J., Finch, J. T. & Thomas, J. O. (1980) *Nature (London)* **287**, 509–516.
7. Baldwin, J. P., Boseley, P. G., Bradbury, E. M. & Ibel, K. (1975) *Nature (London)* **253**, 245–249.
8. Lutter, L. C. (1978) *J. Mol. Biol.* **124**, 391–420.
9. Hayes, J. J., Tullius, T. D. & Wolffe, A. P. (1990) *Proc. Natl. Acad. Sci. USA* **87**, 7405–7409.
10. Srinivasan, A. R. & Olson, W. K. (1988) *J. Mol. Graphics* **6**, 126–134.
11. Jones, T. A. (1978) *J. Appl. Crystallogr.* **11**, 268–272.
12. Ferrin, T. E., Huang, C. C., Jarvis, L. E. & Langridge, R. (1988) *J. Mol. Graphics* **6**, 13–21.
13. van Holde, K. E. (1988) *Chromatin* (Springer, New York).
14. Bavykin, S. G., Usachenko, S. I., Zalensky, A. O. & Mirzabekov, A. D. (1990) *J. Mol. Biol.* **212**, 495–511.
15. Hol, W. G. J., van Duijnen, P. T. & Berendsen, H. J. C. (1978) *Nature (London)* **273**, 443–448.
16. Carter, C. W., Jr. (1978) *Proc. Natl. Acad. Sci. USA* **75**, 3649–3653.
17. Steitz, T. A. (1990) *Q. Rev. Biophys.* **23**, 205–280.
18. Eickbush, T. H. & Moudrianakis, E. N. (1978) *Cell* **13**, 295–306.
19. Musgrave, D. R., Sandman, K. M. & Reeve, J. N. (1991) *Proc. Natl. Acad. Sci. USA* **88**, 10397–10401.